Evaluation of YSZ Ceramic Composite Coating on IS 2062 Steel using Tig Cladding Process for Enhancing Structural Material Performance

[1]K Vema Sai, [2]R Vinay Sai Kumar, [3]D Sai Durga Prasad, [4]Y Dhana Raju, [5]V Praveen Kumar
[1,2,3,4,5] *B. Tech Final Year Student, Department of Mechanical Engineering, Visakha Institute of Engineering and Technology, Visakhapatnam, A.P, India*

Abstract: **This study explores YSZ ceramic coatings on IS 2062 steel via the TIG cladding process at currents from 120A to 200A. Higher currents increase composite layer depth due to enhanced heat transfer. Microstructural analysis shows variations in grain size and dendritic formations with current changes. Coating powder distribution impacts morphology and microstructure. Hardness testing reveals improved hardness in coated substrates, peaking at 120A. Wear rate analysis indicates enhanced wear resistance across currents, with 120A showing the highest resistance, suggesting an optimal processing parameter for durability.**

Index Terms - YSZ ceramic coatings, TIG cladding process, steel substrates, microstructural analysis, grain size, hardness testing, wear resistance.

I. INTRODUCTION

Investigate the application of YSZ ceramic coatings on IS 2062 steel substrates using the TIG cladding process. Analyze the influence of TIG processing current on the depth and uniformity of the composite layer. Examine the microstructure of the coatings, including variations in grain size, dendritic formations, and arm spacing. Investigate the distribution of YSZ coating powder within the coating zone and its impact on coating morphology and microstructure. Evaluate the mechanical properties of the coatings, particularly hardness, using Rockwell hardness (HRC) testing & assess the wear resistance of the YSZ ceramic coatings compared to uncoated steel substrates across various coating currents.

II. RESEARCH METHODOLOGY

The experiment involves preparing steel plates and coating them with a YSZ ceramic composite using a TIG cladding process. Firstly, the steel plates are cut and their surfaces are abraded to ensure good adhesion. The YSZ ceramic powder is mixed with a solution to form a paste, which is then applied onto the substrate. Heat is applied using a TIG torch to melt the coating onto the steel surface. Various TIG currents are used to deposit tracks of the coating onto the substrate. After deposition, the samples are prepared for testing by cutting them into smaller pieces. Testing involves analysing the microstructure and phase constitution using microscopy, measuring the hardness using a Rockwell tester, and assessing the wear rate using a pin-on-disc wear tester. Precautions are taken throughout the process to ensure safety and accurate results, including wearing protective gear, maintaining cleanliness, and documenting observations carefully.

Material Preparation: Steel plates of IS2062 Fe 410 grade were cut to size ($100x50x10mm^3$) and prepared by abrasion for a clean surface. Yttria Stabilized Zirconia (YSZ) microparticles were blended with a solution of polyvinyl alcohol (PVA) and distilled water to form a uniform paste. This paste was then applied onto the prepared steel surface to create a preplaced layer.

TIG Cladding Process: Heat was applied to the preplaced layer using a TIG torch, simultaneously melting the coating and substrate surface. TIG parameters such as electrode diameter, voltage, and scan speed were set, with argon gas supplied to protect the molten metal from oxidation. Different TIG currents ranging from 120A to 200A were used to deposit tracks onto the substrate.

Testing Material Preparation: After curing the preplaced layer, samples were cut into smaller pieces suitable for testing, ensuring uniformity and consistency.

Microstructural & Phase Constitution Characterization: Samples were prepared and observed under inverted optical microscopy to analyse their microstructure. Microhardness and cross-sectional observations were conducted after polishing and etching with Frys reagent.

Rockwell Hardness Testing: Hardness tests were conducted using a Rockwell hardness tester with a 12kg load for 15 seconds dwell time. Fifteen indentations were taken on each sample for accurate readings.

Wear Rate Analysis: Wear tests were conducted using a pin-on-disc wear tester with a 1 kg load and 2000 seconds test duration at a sliding speed of 1m/s.

III. EXPERIMENTAL CONFIGURATION AND TESTING

3.1 Experimental Procedure:

The experimental procedure begins with the preparation of the substrate material, which involves selecting steel plates with grade IS2062 Fe 410 and cutting them into the desired dimensions of 100 x 50 x 10mm³. To ensure a suitable surface for coating adhesion and corrosion resistance, the substrate surface is abraded using 220-grade emery paper. Yttria Stabilized Zirconia Microparticles, with a particle size ranging from 40 to 50 µm, are chosen as the coating powder. These particles are then blended with a solution of polyvinyl alcohol (PVA) and distilled water to form a uniform semisolid solution. This solution is applied to the substrate surface, with the thickness of the preplaced layer maintained at approximately 3mm. After application, the preplaced substrate is allowed to dry at room temperature for 24 hours to remove any moisture.

Next, the TIG (Tungsten Inert Gas) cladding process is employed to melt the preplaced layer and fuse it with the substrate surface. A TIG cladding machine equipped with a tungsten electrode (diameter: 2.4mm) is used for this purpose. The stand-off distance (SOD) between the electrode and the substrate surface is set to 2mm to ensure uniform coating. Argon gas is supplied at a rate of 12 litres per minute to shield the molten metal from oxidation during the cladding process. The TIG current is varied within the range of 120A to 200A, with an increment rate of 20A, while the voltage and scan speed are kept constant at 25V and 3mms^{-1} respectively. After depositing tracks using the specified current settings, any un-melted precursor layer remaining on the substrate is removed. The deposited tracks are then sectioned in transverse cross-sections using wire EDM (Electrical Discharge Machining).

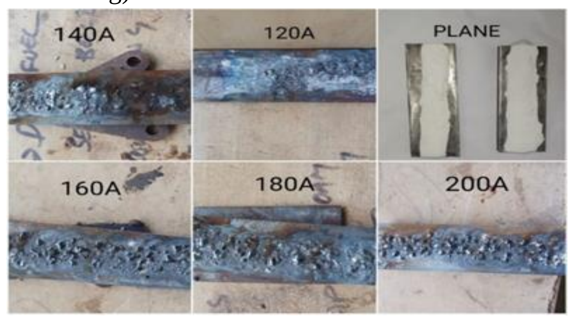

Figure 1: YSZ ceramic coated samples using TIG cladding at various currents

Five tracks processed at different current settings (120A, 140A, 160A, 180A, and 200A) are selected for further investigation of mechanical properties. The TIG heat input for each track is calculated using a formula that considers the thermal efficiency (assumed as 0.48), input voltage, current, and scanning speed. Finally, the welded samples are cleaned, and the better-welded portions are cut for examination of hardness, wear analysis, and microstructure study.

3.2 Testing and Analysis Procedure:

In the testing and analysis procedure, a series of rigorous methods are employed to evaluate the surface performance, microstructure, hardness, and wear behaviour of the YSZ ceramic-coated TIG cladding specimens.

Surface Performance Testing Preparation:

Begin by cutting the YSZ ceramic-coated TIG cladding specimens into dimensions of 40 x 20 x 10mm³ using Wire EDM. This ensures accurate testing and analysis. Prepare the samples according to the specific requirements of each testing method, ensuring they are clean and free from contaminants.

Figure 2: Prepared samples for testing

Microstructural & Phase Constitution Characterization:

Perform microstructure analysis using inverted optical microscopy, which allows for detailed examination of the material's internal structure. Section the selected coated tracks to the proper dimension for characterization, and polish them using silicon carbide (SiC) emery paper followed by alumina paste on micro-cloth. Etch the samples with Frys reagent to enhance metallography observation. Characterize the microstructure of the TIG cladded samples using an optical microscope, adjusting magnification and contrast to visualize fine details. Accurately document observations to facilitate data interpretation and comparison.

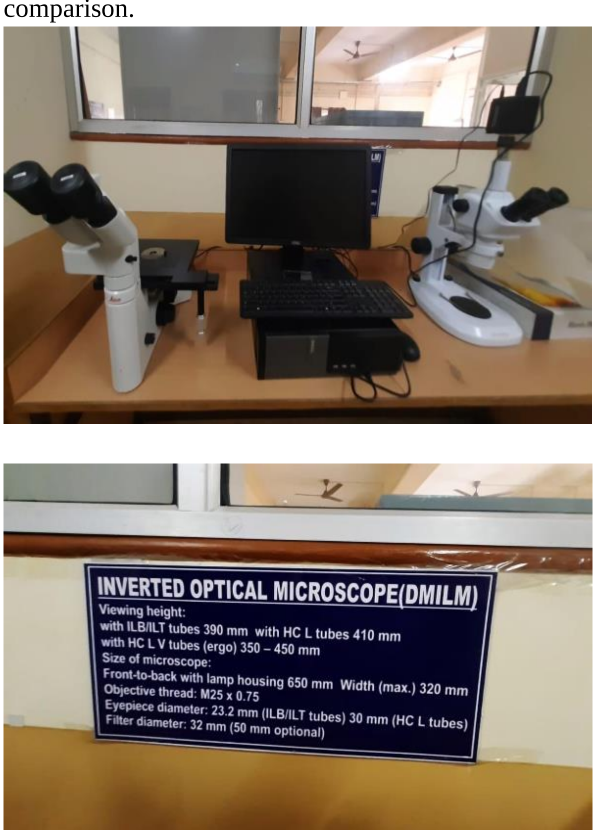

Figure 3 (a) & 3 (b) are the images of Inverted optical microscopy.

Rockwell Hardness Testing:

Conduct Rockwell hardness testing to measure the hardness of the composite coating sample. Apply a 12kg load for a 15-second dwell time and take 15 indentations on every sample from top to bottom for hardness readings. Record HRC values for further investigation, ensuring cleanliness of the surface and proper test conditions.

Figure 4(a), 4(b) & 4(c) are images of Rockwell Hardness Testing

Wear Rate Analysis:

Evaluate wear behaviour through wear tests conducted on both the base metal and coated metal specimens. Utilize a pin-on-disc wear tester with a 1 kg load, conducting wear tests for every specimen for 2000 seconds at a sliding speed of 1m/s. Monitor test parameters such as load, sliding speed, and temperature to ensure consistency and accuracy.

Figure 5: Pin on Disc Wear Testing Machine

Carefully interpret results and compare them with relevant standards to assess the material's wear resistance and performance.

IV. RESULTS AND DISCUSSION

4.1 Microstructure of the Composite Coating

Figure.6 represents the microstructural images in back scattered electron (BSE) mode of the polished samples processed with 120, 140, 160, 180 and 200 A TIG currents. Optical images revealed that the composite layer depth is largely influenced by the TIG processing current. The composite layer depth provides very important information to determine the service life of the components for the tribological application.

Figure.6 indicates the coating depth. After careful observation, it was noticed that the composite layer depth increases with increase in the TIG processing current while other parameters are constant. The main reason for increasing the coating depth is higher heat transfer from the TIG electrode to the substrate. At low processing current low heat input is induced from the electrode which is utilized to melt the precursor layer and very small amount of heat transfer to the substrate resulting in low dilution of the substrate. Whereas, high processing current high heat input induced by the electrode, some amount of heat utilized by the precursor layer and remaining heat transferred to the substrate.

Due to high heat energy absorbed from the precursor layer higher dilution of the substrate occurs. Lower dilution of the substrate is responsible for lower coating depth, whereas higher dilution of the substrate responsible for higher coating depth up to 160 A. Beyond this current the coating depth is decreasing. The coating processed at 120A and 140 A exhibit nearly the same depth. Reason behind this is that at120A processing current, all heat transferred from the electrode absorbed by the precursor layer and the coating materials was not melted properly. Whereas, at 140A processing current the electrode sufficient heat transfer to the precursor layer resulting in melting occurs and very small amount of heat transferred to the substrate. With increasing processing current, the heat density also increases during the deposition of the coating layer resulting in coating depth increase.

Also, during cladding melt pool temperature at the center attains higher value compare to the outer end of the coating. Since, surface tension of the molten pool directly depends on the temperature, the molten YSZ flow within the molten pool of the substrate due to Marangoni fluid flow, this result increases the overall YSZ composite layer depth. Additionally, the lower input current provides low heat energy which leads to low dilution of the composite coating layer with the material of the substrate resulting in low depth of composite layer. While, high processing current provides high heat input that leads to more dilution of the coating materials with the substrate. Hence, processing at 120A current, lower composite layer depth achieved (figure.1(a)); whereas, employing at 160A current, very high depth achieved (figure.1(c)).

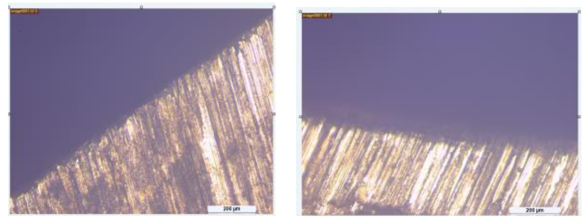

(a) Coating at120A current (b) Coating at 140A current

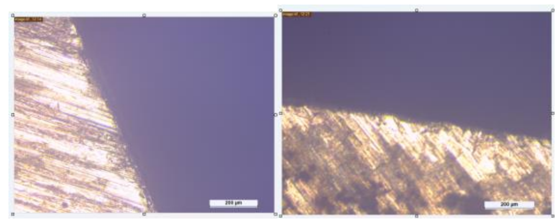

(c)Coating at 160A current (d) Coating at 180A current

(e) Coating at 200A current

Figure 6: Coating thickness with various current values

Figure.7 represents the magnified microstructural images of the cladded samples with processing current 120, 140, 160, 180 and 200 A. It also revealed the distribution of the YSZ coating powder in the coating zone. It is well established that the microstructure of the coating directly depends on the cooling rate, temperature gradient and solidification velocity. These factors control the grain size and formation of the microstructure features.

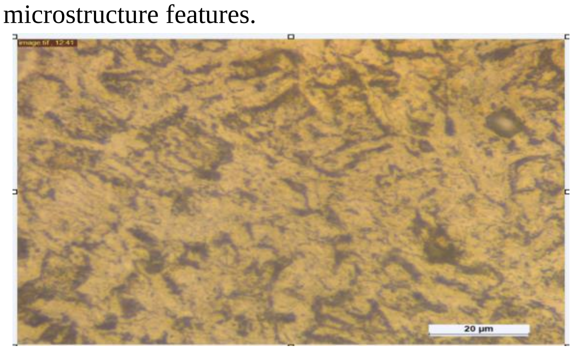

(a)Steel substrate without Coating

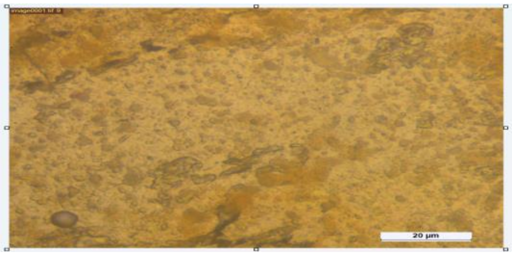

(b) Coating at120A

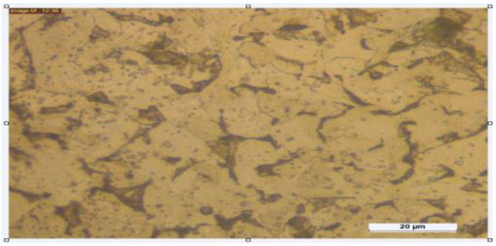

(c) Coating at 140A current

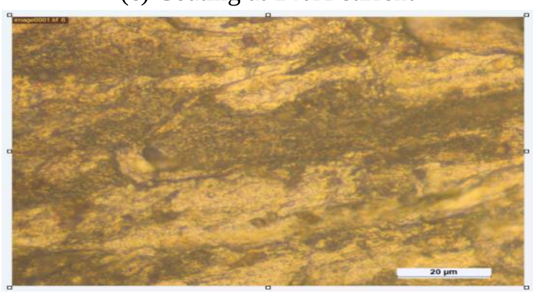

(d) Coating at 160A current

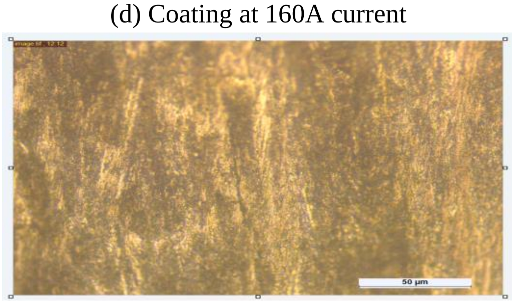

(e) Coating at 180A current

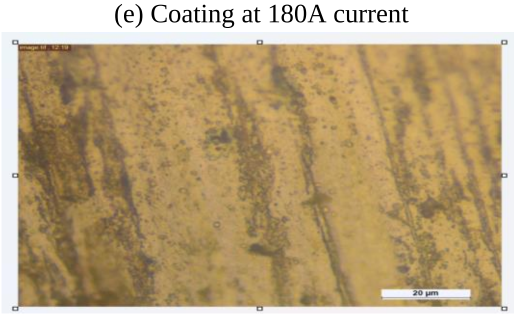

(f) Coating at 200A current

Figure 7: Microstructures of steel substrate coated with YSZ microparticles with various welding currents.

The input current increases from 120 A to 140 A the higher grain refinement of microstructure achieved because of the higher cooling rate acquired at 140A as shown in figures 2(a) and (b). Images also represent the dendrites formation at 140A current as shown in figure 7(b) and above 140 A processing current the dendrites are going to break. Figures 7(a)–(d) also show that arm spacing in the cladded layer, which increases with increase in TIG input current. Hence, it is noticed that the dendritic region decreases with increases in input current due to the dilution of the coating materials with the steel substrate. At very high input current (exceeds from 140A) the dendrite formation decreases and increases the amount of iron (Fe) in the coating due to more dilution of the substrate

4.2 Hardness Measurements

From the Rockwell hardness (HRC) value we observed that compared with uncoated steel substrate, ceramic coated steel substrate hardness improved & maximum hardness obtained for steel substrate with coating at 120A current i.e. 1.29 times greater than uncoated steel substrate. Also observed that, when current of coating increased then hardness of steel substrate was decreased. Refer the below Table-2, Graph-1 & Chat-1 for the variation of hardness values respective of welding currents during coating.

Table 1**.** Rockwell hardness values at various coating currents

COATING CURRENT	HRC			AVERAGE HARDNESS
	READING 1	READING 2	READING 3	
UNCOATED	26.6	31.3	32	29.967
120A	41.6	38.9	35.5	38.667
140A	27	35	34	32.000
160A	23.9	35.7	36	31.867
180A	29.5	31.8	35.1	32.133
200A	34.1	27.8	28.8	30.233

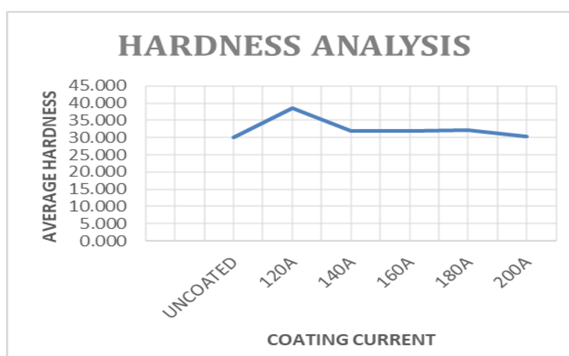

Figure 7: HARDNESS ANALYSIS

4.3 Wear Rate Analysis

From the wear rate analysis, we can conclude that there was an improvement in wear resistance by YSZ ceramic coating. Compared to uncoated steel substrate we can see 1.3 to 2.5 times wear decreased at various coated currents. While compared with coated substrate more wear rate is decreased in steel substrate coated at 120A i.e. 2.5 times and observed that increasing in wear rate with respect to the increase in coating current. Refer the below Table-3, graph-2 & chat-2 for the variation of hardness values respective of welding currents during coating.

Table 2. Wear Analysis at various coating currents

WEAR ANALYSIS		
CURRENT	AVERAGE WEAR (mm)	WEAR RESISTANCE ACHIEVED (times)
UNCOATED	0.005	0.0
120A	0.002	2.50
140A	0.0036	1.39
160A	0.0035	1.43
180A	0.0032	1.56
200A	0.003	1.67

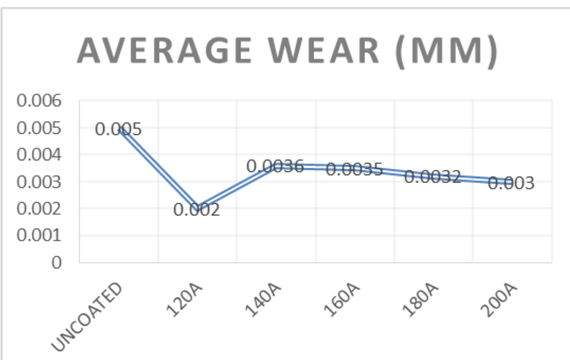

Figure 8: Average wear rate at various coating currents

V. CONCLUSION

5.1 Conclusion

In conclusion, the experimental investigation into TIG-clad YSZ ceramic coatings on steel substrates yielded valuable insights into the effects of processing parameters on coating properties. The study demonstrated that higher TIG processing currents resulted in increased coating depth but also led to decreased hardness and wear resistance beyond a certain threshold.

The microstructural analysis revealed finer grain structures at higher currents, indicating enhanced cooling rates, while wear rate analysis showed substantial improvements in wear resistance with ceramic coatings, particularly at lower processing currents.

These findings highlight the intricate relationship between TIG processing parameters and coating properties, emphasizing the need for careful optimization to achieve desired performance characteristics. Future research could focus on further refining processing parameters to maximize coating effectiveness and durability in practical applications, ultimately contributing to the advancement of surface engineering techniques for enhanced material performance and longevity.

5.2 Future Scope

This study lays the groundwork for further exploration in the field of YSZ ceramic coatings on steel substrates via the TIG cladding process. Future research could focus on optimizing processing parameters to achieve an ideal balance between coating depth, hardness, and wear resistance. Additionally, there's potential for investigating alternative ceramic materials and composite formulations to enhance coating performance. Application-specific studies across different industries can help assess the coatings' suitability for various environments, while advanced characterization techniques may offer deeper insights into their microstructural evolution. By addressing these areas, future research can contribute to advancing the development and application of YSZ ceramic coatings for improved performance and durability in real-world scenarios.

VI. REFERENCES

[1] Kaushik Biswas and Chinmaya Kumar Sahoo "A review on TIG cladding of engineering material for improving their surface property,"2023 Surf. Topogr.: Metrol. Prop. 11 023001

[2] Sujeet Kumar and Anil Kumar Das "Evaluation of mechanical properties of TiB2 -TiO2 ceramic composite coating on AISI 1020 mild steel by

TIG cladding”,2022 Eng. Res. Express 4 015034
[3] Anil Kumar Das “Recent developments in TIG torch assisted coating on austenitic stainless steel: A critical review,” https://doi.org/10.1016/j.matpr.2022.01.077
[4] Haojun Wang, Tao Chen, Weilong Cong, and Defu Liu “Laser Cladding of Ti-Based Ceramic Coatings on Ti6Al4V Alloy: Effects of CeO2 Nanoparticles Additive on Wear Performance”, *Coatings* 2019, *9*(2), 109; https://doi.org/10.3390/coatings9020109
[5] Balamurugan Sivaramakrishnan &Murugan Nadarajan “A Study on Microhardness, Microstructure and Wear Properties of Plasma Transferred Arc Hard faced Structural Steel with Titanium Carbide”10.4236/jmmce.2014.23020
[6] Ji R, Liu Y, Zhang Y, Cai B, Li X and Zheng C 2013 Effect of machining parameters on surface integrity of silicon carbide ceramic using end electric discharge milling and mechanical grinding hybrid machining J. Mech. Sci. Technol. 27 177–83
[7] E A S Almeida, C E da Costa et al. “Microstructural and tribological characterization of niobium boride coating produced on AISI 1020 steel via multicomponent boriding A P Krelling”
[8] Xinhong W, Lin C, Min Z and Zengda Z 2009 Fabrication of multiple carbide particles reinforced Fe-based surface hard facing layer produced by gas tungsten arc welding process Surf. Coat. Technol. 203 976–80
[9] Du B, Zou Z, Wang X and Qu S 2008 Laser cladding of in situ TiB2/Fe composite coating on steel Appl. Surf. Sci. 254 6489–94
[10] Lin Y C and Liu Y 2020 Effects of Co and W on the microstructure and wear behaviour of NiCrAlMoTiFeNbX equimolar multicomponent-clad layers Wear 446 203186
[11] Masanta M, Shariff S M and Choudhury A R 2011 A comparative study of the tribological performances of laser clad TiB2–TiC–Al2O3 composite coatings on AISI 1020 and AISI 304 substrates Wear 271 1124–33
[12] Sahoo C K and Masanta M 2015 Effect of pulse laser parameters on TiC reinforced AISI 304 stainless steel composite coating by laser surface engineering process Opt. Lasers Eng. 67 36–48
[13] B. Heidarshenas, G. Hussain, M. Asmael, Development of a TiC/Cr23C6 Composite Coating on a 304 Stainless Steel Substrate through a Tungsten Inert Gas Process, Coatings 7 (6) (2017) 80, https://doi.org/ 10.3390/coatings7060080
[14] Sahoo, C.K.M. Masanta, Microstructure and mechanical properties of TiC-Ni coating on AISI304 steel produced by TIG cladding process, J. Mater. Process. Technol. 240 (2017) 126–137, https://doi.org/10.1016/j. jmatprotec.2016.09.018